(2)

TECHNICAL REPORT BRL-TR-3328

BRL

MULTICOMPONENT COMPARISON OF OPTICAL AND MASS SPECTROMETRIC DIAGNOSTICS IN LOW-PRESSURE FLAMES

STEPHEN L. HOWARD
RANDY J. LOCKE
DAVID C. DAYTON
ROSARIO C. SAUSA
ANDRZEJ W. MIZIOLEK

APRIL 1992

U.S. ARMY LABORATORY COMMAND

BALLISTIC RESEARCH LABORATORY
ABERDEEN PROVING GROUND, MARYLAND

NOTICES

Destroy this report when it is no longer needed. DO NOT return it to the originator.

Additional copies of this report may be obtained from the National Technical Information Service, U.S. Department of Commerce, 5285 Port Royal Road, Springfield, VA 22161.

The findings of this report are not to be construed as an official Department of the Army position, unless so designated by other authorized documents.

The use of trade names or manufacturers' names in this report does not constitute indorsement of any commercial product.

REPORT DOCUMENTATION PAGE

Form Approved
OMB No. 0704-0188

1. AGENCY USE ONLY (Leave blank)	2. REPORT DATE	3. REPORT TYPE AND DATES COVERED
	April 1992	Final Oct 1989 - Oct 1991

4. TITLE AND SUBTITLE

Multicomponent Comparison of Optical and Mass Spectrometric Diagnostics in Low-Pressure Flames

5. FUNDING NUMBERS

PR: 1L161102AH43

6. AUTHOR(S)

Stephen L. Howard, Randy J. Locke, David C. Dayton, Rosario C. Sausa, Andrzej W. Miziolek

7. PERFORMING ORGANIZATION NAME(S) AND ADDRESS(ES)

U. S. Army Ballistic Research Laboratory
ATTN: SLCBR-IB-P
Aberdeen Provind Ground, MD 21005-5066

8. PERFORMING ORGANIZATION REPORT NUMBER

9. SPONSORING/MONITORING AGENCY NAME(S) AND ADDRESS(ES)

U. S. Army Ballistic Research Laboratory
ATTN: SLCBR-DD-T
Aberdeen Provind Ground, MD 21005-5066

10. SPONSORING/MONITORING AGENCY REPORT NUMBER

BRL-TR-3328

11. SUPPLEMENTARY NOTES

12a. DISTRIBUTION/AVAILABILITY STATEMENT

Approved for Public Release; Distribution Unlimited

12b. DISTRIBUTION CODE

13. ABSTRACT *(Maximum 200 words)*

A new generation of flat flame burner system for characterization of one-dimensional premixed laminar flames has been developed to study the detailed flame chemistry relevant to gaseous flames of burning propellants. This instrument incorporates several spectral techniques in one apparatus so that various diagnostic techniques can be quantitatively compared and the usable detection range (both in terms of spatial resolution and species detection) expanded. Features include molecular beam sampling with triple quadrupole mass spectrometric detection (MB/MS), laser-induced fluorescence (LIF), resonance-enhanced multiphoton ionization (REMPI), and temperature analysis by thermocouple and LIF. The intercomparison of different diagnostic techniques was accomplished on a stoichiometric 20 Torr $C_2H_4/O_2/Ar$ flame. Profiles for O, H, and OH were obtained. Temperature profiles were taken of the unperturbed as well as perturbed (quartz sampler present) flames. As expected, the quartz sampler acted as a heat sink (approximately 200 K lower in the highest temperature flame regions). In general, the comparison between the different diagnostic techniques, is fair. Possible reasons for the minor discrepancies observed are discussed and include diffusion and thermal effects for the mass spectrometric technique as well as photochemical and stimulated emission effects for the laser diagnostics.

14. SUBJECT TERMS

Premixed, Laminar Flames; Low-Pressure Burner; Collision-Induced Dissociation; Laser Induced Fluorescence; Resonance-Enhanced Ionization; Mass Spectrometry

15. NUMBER OF PAGES

35

16. PRICE CODE

17. SECURITY CLASSIFICATION OF REPORT	18. SECURITY CLASSIFICATION OF THIS PAGE	19. SECURITY CLASSIFICATION OF ABSTRACT	20. LIMITATION OF ABSTRACT
UNCLASSIFIED	UNCLASSIFIED	UNCLASSIFIED	UL

INTENTIONALLY LEFT BLANK

TABLE OF CONTENTS

INTENTIONALLY LEFT BLANK

LIST OF FIGURES

LIST OF TABLES

INTENTIONALLY LEFT BLANK

ACKNOWLEDGEMENTS

We would like to thank the Office of Naval Research (ONR Contract No. 00001491MP24001) and the BRL combustion Research mission program for funding of this work. Purchase of equipment through the Productivity Capital Investment Funds is gratefully acknowledged. Support of Stephen L Howard, Randy J. Locke and David C. Dayton by the National Research Council Research Associate Program is also gratefully acknowledged. We would also like to thank Professor T. A. Cool and his student J. S. Berstein, Cornell University, for numerous helpful discussions and useage of their REMPI power supply filter.

Randy J. Locke is currently employed at:

Sverdrup Technology, Inc.
LeRC Group
Mailstop SVR-2
2001 Aerospace Parkway
Brook Park, OH 44142.

INTENTIONALLY LEFT BLANK

1. INTRODUCTION

A good deal is yet unknown about the actual reaction mechanisms in propulsion flames. It is becoming increasingly important that such mechanisms are known. Propellant selection and optimization are dependent upon burning characteristics and the products formed. Much modeling effort has been expended in an attempt to understand these processes. However, experimental results upon which these models are based vary with different diagnostic methods and flame conditions.

Over the past few decades, there has been significant progress in the study of the structure of flames. Several laser spectroscopic techniques such as laser-induced fluorescence (LIF) and multiphoton techniques such as resonance-enhanced multiphoton ionization (REMPI) have yielded species concentration measurements with a good degree of selectivity and spatial resolution (Lucht et al. 1983, Alden et al. 1982, Goldsmith 1983). Flame temperatures have also been measured by LIF of the OH radical employing its well-known $A\,^2\Sigma^+ \leftarrow X\,^2\Pi_i$ (1,0) band near 281 nm. The OH radical has been the subject of many studies since it is ubiquitous in most flame systems and can be modeled spectroscopically. However, there is evidence that strong photon flux at short wavelengths can photolyze other major flame species and produce anomalously high local concentrations of radicals such as O-atom that strongly perturb local temperatures and concentrations of other trace species (Goldsmith 1987, Miziolek and DeWilde 1984). More physically intrusive techniques such as gas-liquid chromatography (GC) or mass spectrometry have also been used (Eltenton 1947, Serry and Zabielski 1989, Banna 1979, Foner and Hudson 1953, Greene et al. 1964, Homann et al. 1963, Biordi et al. 1973, Biordi et al. 1974, Vandooren et al. 1974, Balakhnin et al. 1977, Puechberty and Cottereau 1983). As with the laser-based techniques, these techniques have advantages for some flame species and flame conditions and disadvantages for others. One experimental technique that has proven to be particularly useful is molecular beam mass spectroscopy (MB/MS) (Foner and Hudson 1953, Greene et al. 1964, Homann et al. 1963, Biordi et al. 1973, Biordi et al. 1974, Vandooren et al. 1974, Balakhnin et al. 1977, Puechberty and Cottereau 1983, Revet et al. 1978).

Use of the supersonic expansion in forming the molecular beam effectively "freezes out" the chemistry of the sampled volume, thus leading to the detection of both

stable and reactive species. In principle, the MB/MS technique should be the preferred tool for flame structure studies since it can detect all major stable species, both reactants and products, as well as all major radical species. Unfortunately, the insertion of the quartz sampler into the flame regions leads to perturbation of the flow fields and local temperatures. This deficiency was recognized early and considerable effort has been expended towards quantifying the extent of the flame perturbation and assessing its impact on experimentally measured temperature and species profiles (Biordi et al. 1974, Revet et al. 1978, Smith 1981, Colket, III et al. 1982 Smith and Chandler 1986). In general, a number of previous studies have concluded that the flame perturbation, though measurable and not insignificant, was usually not so great as to make use of the species profiles misleading (Revet et al. 1978, Biordi et al. 1973). However, this issue is not completely resolved, and is still an active area of experimental concern.

One of the difficulties in ascertaining the degree of probe perturbation is the fact that whenever comparisons have been made between MB/MS and other flame diagnostic techniques, they have been made with only one or two flame species (Biordi et al. 1973, Smith and Chandler 1986, Rosier et al. 1988), despite the fact that it is well-recognized that every flame diagnostic technique suffers from some kind of deficiency. For example, LIF and REMPI are generally only applicable to 1-3 atom size molecules which have a well-defined and understood ultraviolet-visible absorption spectrum. In addition, LIF requires strong to moderate fluorescence. The bulk of flame species, particularly stable reactants and flame products, are not amenable to this type of detection. Other LIF problems include the quantification of the fluorescence signal. The signal is affected by collisional quenching by various species in the flame and whose rate constants are generally unknown (Cattolica and Mataga 1991) and by possible photochemical effects - particularly when the necessary laser probe wavelengths are in the ultraviolet region and/or multiphoton processes are accessed.

Other optical diagnostic techniques such as Fourier-transform infrared (FTIR) and tunable diode laser (TDL) absorption spectroscopies are affected by line-of-sight considerations. In view of this situation, an apparatus such as the low-pressure burner described in this report was developed such that each mentioned flame diagnostic is available so that its strengths and weaknesses under the same experimental conditions can best be ascertained. In this report we describe flame concentration profiles of H,

O, and OH obtained from a stoichiometric 20 Torr $C_2H_4/O_2/Ar$ flame utilizing MB/MS, LIF, and REMPI techniques.

2. EXPERIMENTAL

The flames were supported on a commercial flat burner inside the low-pressure chamber as shown in the schematic of the apparatus in Figure 1. Under proper gas flow conditions the flame was one-dimensional with respect to the burner surface. In order to increase the spatial resolution the flame was operated at reduced pressure. Studies of low-pressure (or subatmospheric) flames have shown that the reaction zones expand with minimal distortion as pressure is reduced (Gaydon and Wolfhard 1949, Salmon and Laurendeau 1987). All of the flames in this report were operated at 20 Torr absolute pressure. Flow rates of C_2H_4, O_2 and Ar were 0.4, 1.2 and 2.8 standard liters/minute, respectively.

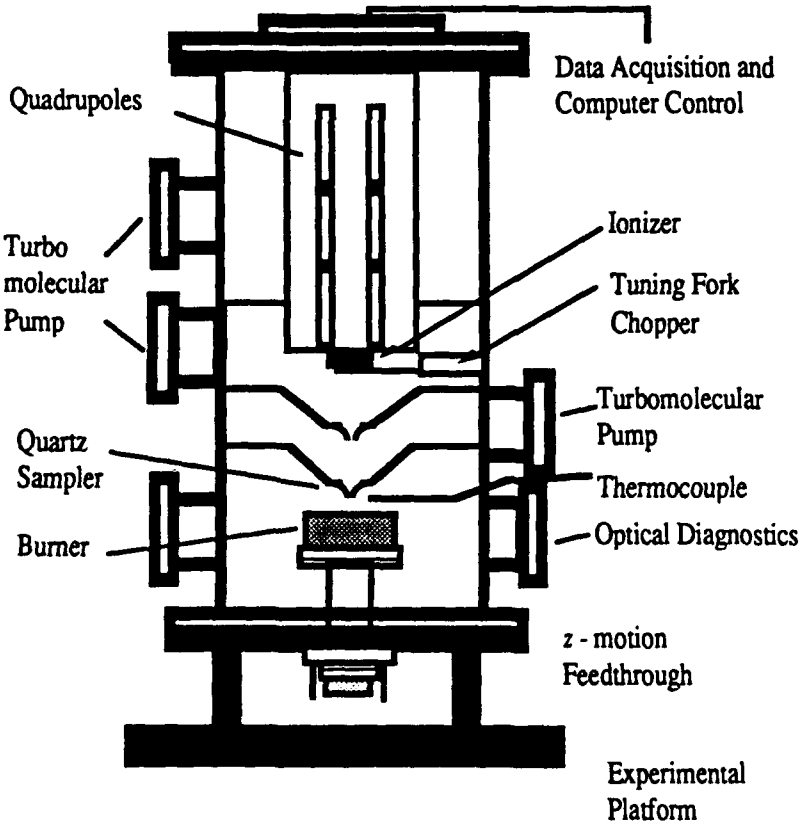

Figure 1. Schematic of Triple Quadrupole Mass Spectrometer and Molecular Beam System of the Experimental Apparatus.

The vacuum chamber consisted of a stainless steel cylinder with an inside nominal diameter of 25 cm and a height of 40 cm which can be easily evacuated to less than 1 Torr using a 50-cfm direct drive vacuum pump. Typically, the chamber pressure is in the 5-50 Torr range for the flames studied to date and was maintained with a baratron pressure gauge with pressure controller. As shown in Figure 1 various observation ports were placed in locations convenient to the placement of laser beams and detectors. This arrangement, of necessity, required optical measurements be obtained in the lower portion of the chamber and MB/MS measurements in the upper portion (the quartz sampler is rigidly attached to the chamber separator cone). In order to access these two positions, the burner was mounted on a x-Θ translation stage that allowed horizontal centering of the burner (accuracy to within one degree) and z-motion (scanning the distance between the diagnostics and the burner surface). The translation stage permitted the diagnostics to remain stationery as the burner was scanned (vertical precision of less than 50 micron) during the profile measurements. The burner was water cooled to maintain a constant temperature as measured by imbedded Alumel-Chromel thermocouples.

The reactant gases were of commercial high-purity grade and were metered by mass flow controllers (calibrated with a wet test meter) and premixed in the burner prior to passing through the flat 6-cm diameter sintered stainless steel plug in the center of the burner surface. Gas flow rates for C_2H_4, O_2 and Ar of 0.4, 1.2 and 2.8 liter/minute (STP), respectively, were used which resulted in linear flow velocities on the order of 120 cm/second, well within the laminar regime (Reynolds number of 110).

The schematic for the layout of the laser-based diagnostics is given in Figure 2. The excimer-pumped dye laser system equipped with second harmonic generation provided laser radiation both in the visible and ultraviolet. The laser beam was then focussed over the center of the burner with 30- to 100-cm focal length lenses.

Laser-induced fluorescence was collected orthogonally to the excitation laser beam and focussed with a 300-mm focal length lens onto the image plane of the photomultiplier after passing an appropriate interference filter. The signal was then fed into a boxcar integrator set for a 9-nsec gate (the short gate minimized the effect of collisional quenching and/or energy transfer of the rotationally excited states) and

plotted on a strip-chart recorder or fed to a digital oscilloscope (500 MHz) and PC-type computer for recording. All LIF signals were obtained in the unsaturated regime so therefore the laser probe energy was monitored by a photodiode and used to normalize the signal. The REMPI signal was collected by the optogalvanic probe (an electrically insulated 0.5 mm diameter platinum rod with an exposed tip as shown in Figure 3a). The charge was detected as a voltage pulse across a 10 kΩ resistor connected between the probe and the negative bias voltage source (the anode for the circuit is the grounded burner). The pulses with 15 μs decay were then amplified with a Tektronix 504 differential amplifier. Flame micophonics were minimized with bandpass (10 KHz to 1 MHz) filtering. The signal was then processed in like manner as the LIF signal.

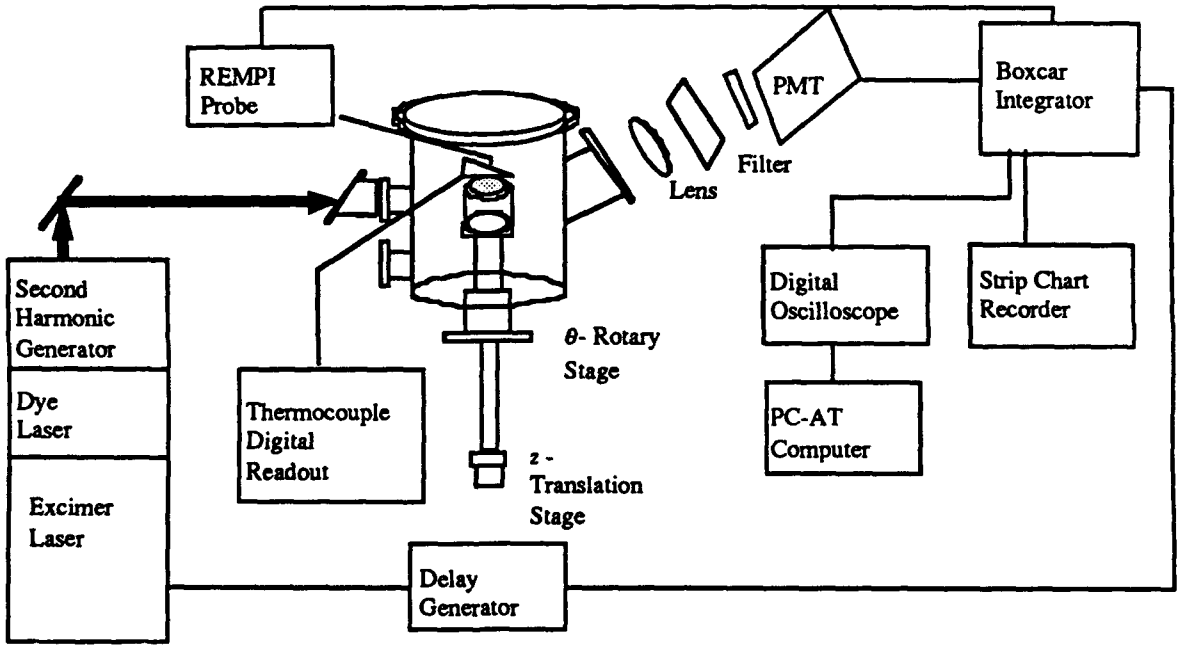

Figure 2. Schematic of Laser-Based and Thermocouple Diagnostics of the Experimental Apparatus.

Thermocouples were employed for flame temperature measurements. The thermocouple consisted of 125 micron diameter platinum/platinum-10% rhodium wires spot welded together to form a junction and coated with a noncatalytic beryllium/yttrium oxide mixture (Kent 1970). As shown in Figure 3b the thermocouple wire was then spot welded to the opposing arms of a V-shaped probe, one arm of which was spring loaded to remove sag as the wire length changed with temperature. The thermocouple was also corrected for radiation loss by using a measured diameter of 190 micron for

the coated thermocouple junction and 0.6 for the emissivity. Comparison with previous OH rotational LIF temperature measurements indicates an uncertainty better than ±50 K in the region of peak temperatures (Sausa et al. 1991).

The mass spectrometer consisted of an Extrel C50 TQMS inline triple quadrupole mass filter with a concentric-axis ionizer as shown schematically in Figure 1. Flame gases were prepared by sampling the flame through a conical quartz skimmer with a 250 micron (approximate) diameter orifice. The gases expanded supersonically into the first differential vacuum chamber with a background pressure of 5×10^{-5} Torr. The expanding gases were then formed into a supersonic beam by collimation through

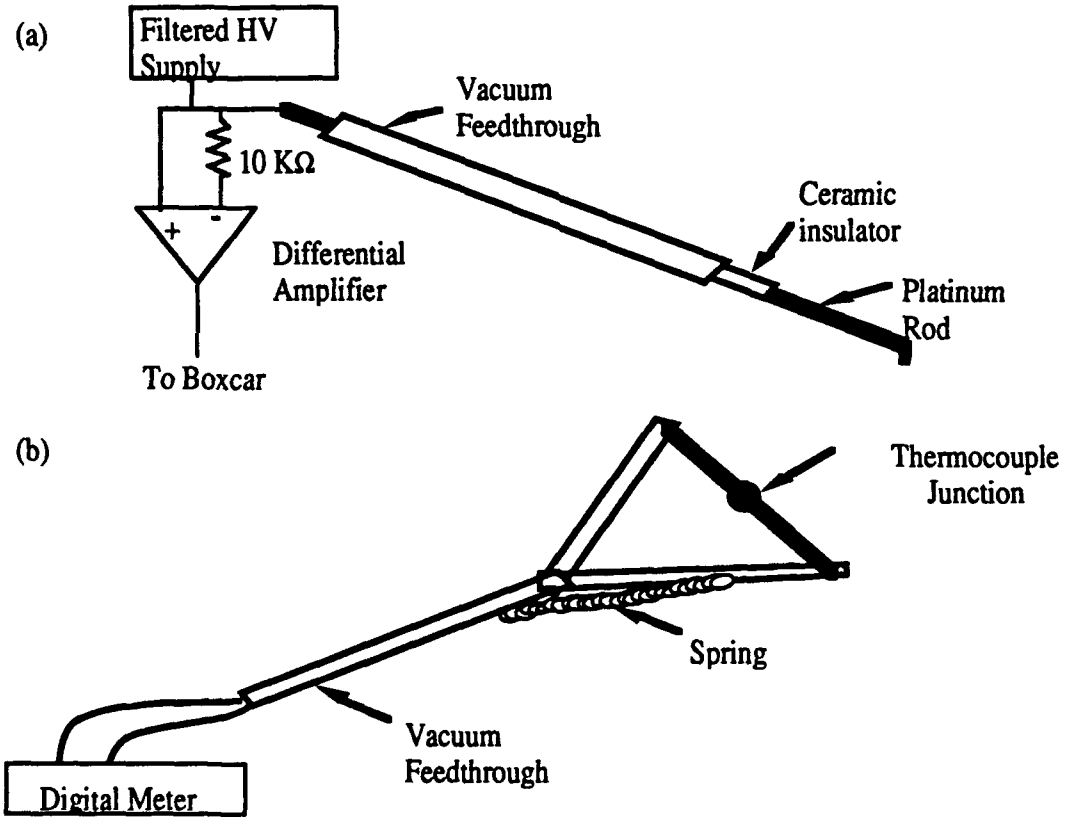

Figure 3. Schematic of (a) REMPI Probe and (b) Thermocouple Probe.

a second skimmer and into the ionization region of the first quadrupole maintained at 2 x 10^{-6} Torr. The beam was then modulated at 200 Hz with a tuning fork chopper and ionized prior to entering the first quadrupole. The electron emission current was maintained at 0.10 ±0.01 mA and the nominal energy at 17.0 ±0.1 eV unless otherwise noted. The drawout voltage from the ionizer was set at less that 1 Volt. These ionizing conditions optimized and stabilized the modulated beam. A beamstop was included to determine if the modulated beam was a molecular beam (modulation would cease with beamstop activated) or an effusive beam (no change in modulation noted with beamstop activated). The low ionization energy avoided dissociation of H_2O present as background or as a major flame product.

For ions that could be assigned unambiguously the triple quadrupole was operated as a single quadrupole with mass filtering by either the first or third quadrupole. For ions that required further identification by collision-induced dissociation (CID), the first quadrupole selected ions of interest in the ionized beam. These ions were then passed through the rf-only quadrupole where collision with argon maintained at a pressure of 10^{-3} Torr occurred. Upon collision, selected ions fragmented and the daughter fragments were analyzed in the third quadrupole. In both cases (with/without CID), after traversing the quadrupoles the ion current was detected with a continuous-dynode electron multiplier. Amplified current from the detector then was processed with a lock-in amplifier. Phase sensitive detection allowed discrimination of background gases and signal averaging to increase sensitivity.

3. RESULTS AND DISCUSSION

3.1 Temperature Measurements. As mentioned in the Experimental Section, the thermocouples were corrected for radiation loss. Temperature correction from radiation loss by the thermocouple junction was approximated by equating the heat transferred to the thermocouple from the gases to that lost by radiation. The corrective term is given by (Hayhurst and Kittelson 1977, Peterson 1981)

$$\Delta T = T_{cal} - T_{obs} = \varepsilon\sigma d(T_{obs}^4 - T_o^4)/2k \qquad (1)$$

where ϵ is the emissivity of the coated thermocouple [taken to be 0.6 (Peterson 1981)], σ is the Stefan-Boltzmann constant, d is the diameter of the coated junction, k is the thermal conductivity of the gases present at the sampling region (usually approximated with values for air) and T_0 is approximately 300 K. The actual thermal conductivity at each point in the flame was obtained as a function of temperature using empirical expressions (Liley and Gambill 1973) and corrected for gas composition as measured in this study. The value of k for the gas mixture varied from 8.41×10^{-5} to 4.09×10^{-4} cal sec^{-1} cm^{-1} K^{-1}. The uncertainty in temperature measurements was estimated to be 50 K in the region of peak temperature and 10 K in the preheat region.

The thermocouple was mounted in two positions. The first position was at the level of the laser diagnostics and the second was to within 1 mm in the radial dimension of the quartz sampler tip at the same horizontal location of the orifice opening. Temperature measurements in the flame at both positions are presented in Figure 4. It shows approximately 200 K decrease in the region of highest temperature at the same location in the flame when the quartz sampler was present. In the preheat region and near the burner surface the temperatures were nearly the same. These results are

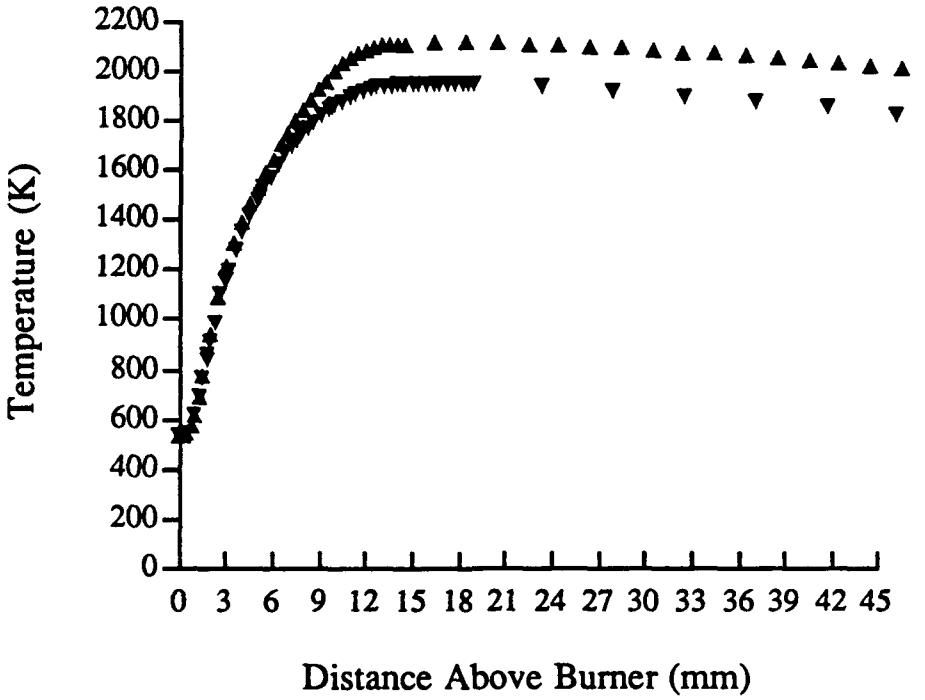

Figure 4. Temperature Profile of Stoichiometric $C_2H_4/O_2/Ar$ Flame at 20 Torr Without Quartz Sampler (▲), is Compared with that Obtained with Quartz Sampler in Flame (▼).

contrasted with previous studies where nearly constant temperature differences were observed throughout the flame zone (Biordi et al. 1973, Smith and Chandler 1986). The reason for the difference between studies is not clear at this time, but undoubtedly is due to specifics of heat transfer due to quartz sampler and burner geometries and to flame operating conditions.

3.2 Spectroscopic Measurements. All species were measured by molecular beam mass spectrometry. The optical diagnostic, however, varied with each species measured. The different optical spectroscopic diagnostics are given in Table 1. H-atom concentration was obtained by REMPI excitation near 243 nm, O-atom by LIF near 223 nm, and OH by LIF near 281 nm. OH radical has been the subject of many LIF studies because its spectrum is well-known and the ($A\ ^2\Sigma^+ - X\ ^2\Pi$) transition is

Table 1. Detection Schemes Employed for Species Profiling (LIF and REMPI)

Species	Excitation Wavelength	Transition	Emission Wavelength	Transition
OH	281 nm	($A\ ^2\Sigma^+ \leftarrow X\ ^2\Pi$) (1,0)	313 nm	(1,1) band
O	225.6 nm	$2p^3 3p\ ^3P \leftarrow 2p^4\ ^3P$	844.7 nm	$2p^3 3p\ ^3P \rightarrow 3s\ ^3S$
H	243 nm	$2s \leftarrow 1s$	N/A	(2+1) REMPI

easily accessible in the near ultraviolet. This radical is a simple diatomic which can be modeled spectroscopically. It also appears to be ubiquitous in flame systems and play a major role in reaction mechanisms.

Figure 5 shows the LIF excitation spectrum of the OH ($A\ ^2\Sigma^+ - X\ ^2\Pi$) (1,0) band near 281 nm taken approximately 7 mm above the burner surface. The probe laser intensity was attenuated in order to avoid saturation of the rotational transitions. Fluorescence intensity measurements of several rotational lines as a function of laser power yielded an energy dependence of one; thus, indicating that saturation did not occur. During these measurements it was decided that the (1,0) band was more useful than the stronger (0,0) band near 306 nm. This spectral region is less congested and self absorption is minimized (self absorption can distort intensity relationships and also prevent a local thermal equilibrium from being established).

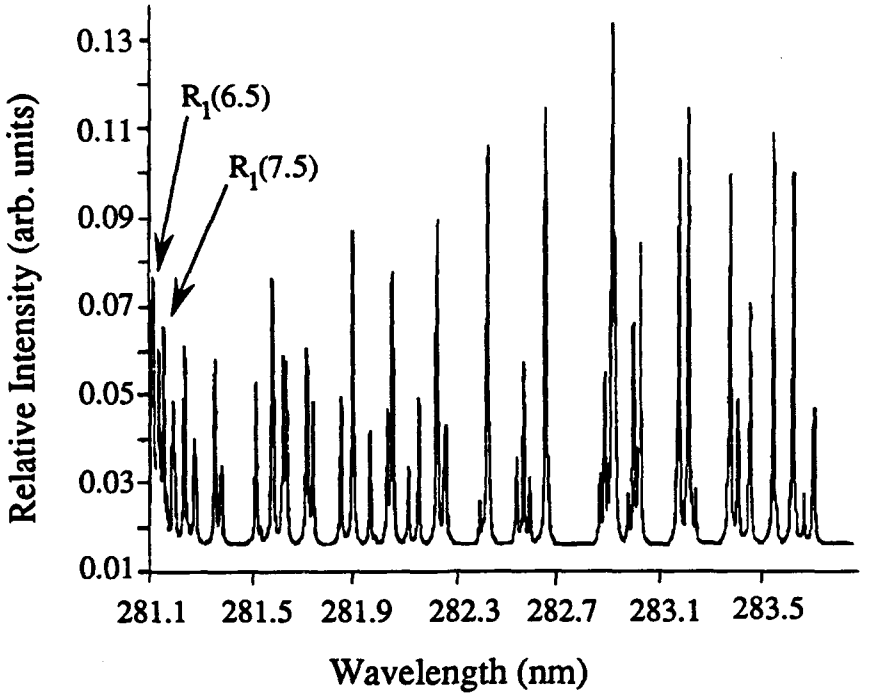

Figure 5. Rotational Spectra of the OH ($A\ ^2\Sigma^+ - X\ ^2\Pi$) (1,0) Band Near 281 nm for the $C_2H_4/O_2/Ar$ Flame at 20 Torr. Spectrum was Taken Near 6 mm Above Burner Surface. Rotational Temperature is Calculated at 1540 ±50 K.

The experimental OH concentration profile was obtained by monitoring rotational transitions relatively insensitive to temperature variations. These transitions were calculated by the following relation (Eckbreth 1988):

$$J^2 + J - (k_B/hcB_v)T_{av} = 0 \qquad (2)$$

where J is the rotational level, k_B, h, c, B_v spectroscopic constants and T_{av} the average flame temperature. Both the J = 6.5 and 7.5 lines of the R_1 branch of the (0,1) transition were monitored and found to give equivalent results. For O-atom, the J = 2 excitation line of the ground state was monitored.

3.2.1 H-atom. Figure 6 shows the H-atom profiles obtained using MB/MS and REMPI (see Table 1). Since it is very difficult to directly quantify radical species

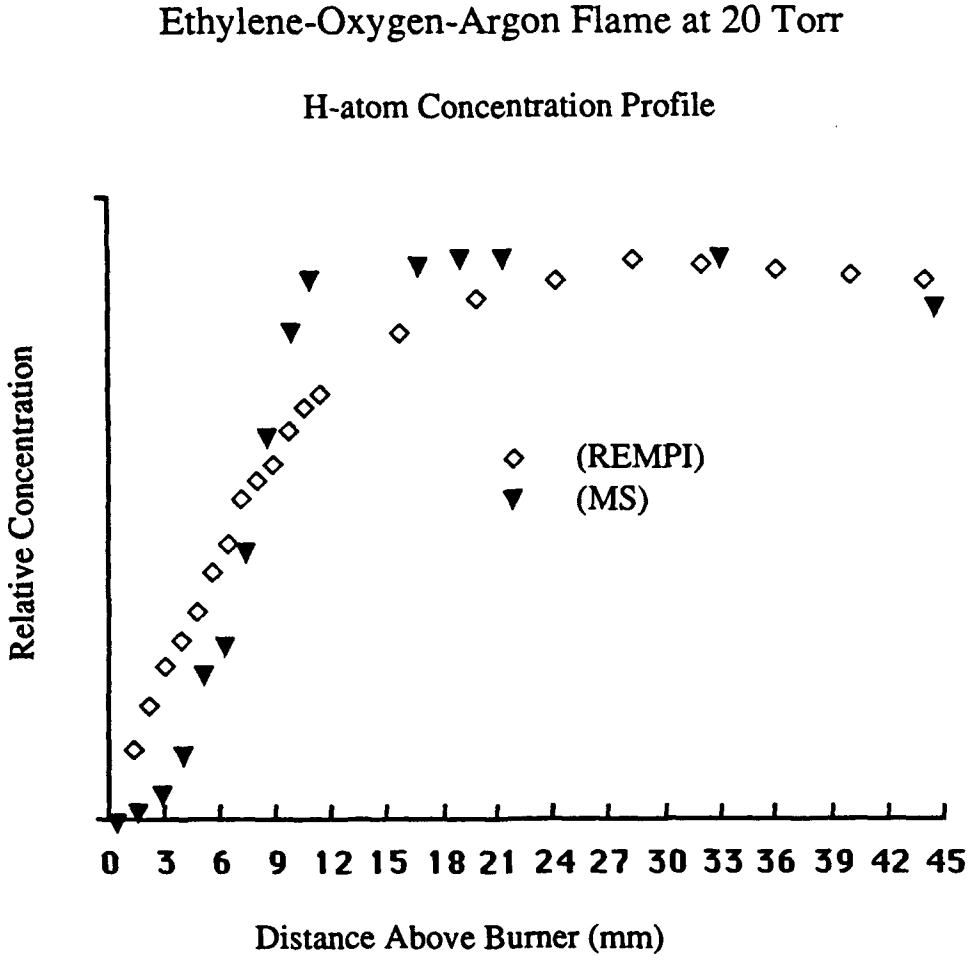

Figure 6. Species Profiles of Stoichiometric $C_2H_4/O_2/Ar$ Flame at 20 Torr. H-Atom Obtained by REMPI (◇), is Compared with that Obtained by Mass Spectrometry (▼).

such as H-atom, O-atom or OH with any of the experimental techniques available on the instrument, the experimental profiles shown in Figures 6-8 are normalized to a unity. In general, agreement between these two experimental techniques is quite good. In the preheat region of the flame the REMPI profile "leads" the MB/MS profile. This result is expected within the region of 0-3 mm above the burner surface since it has been previously observed that with the quartz probe near the burner surface a lower concentration of radicals is observed due to the probe's interference in the process of backward (toward the burner surface) diffusion (Revet et al. 1978). It is also expected that radical, flame intermediates and product concentrations measured with the probe nearly touching the burner surface (approximately 0 mm above the surface) will be zero

since the physical presence of the probe precludes the possibility of these species within the sampled volume.

The REMPI profile drops somewhat below that obtained by MB/MS in the region of the primary flame zone. This result may be the due to very large quenching rates of the REMPI intermediate (two-photon) excited H(2p) state with other flame intermediates prior to absorbance of the third photon and subsequent ionization (Goldsmith et al. 1982, Bittner et al. 1988). It is also likely that the REMPI results in the preheat zone (prior to 7 mm) may also be augmented by fuel and/or oxidizer photolysis at the laser wavelength of 243 nm. In general, this possibility of photochemical perturbation becomes a greater concern the larger the hydrocarbon species present in the flame. As a matter of experimental protocol, the desired approach of using high pulse energies to keep the photoionization rate high to minimize quenching effects directly conflicts with the requirement to keep extraneous photochemical effects low (low pulse energies) and thus complicates this diagnostic technique. This possible problem and its extent are presently under detailed study.

3.2.2 OH Radical. OH radical has been the subject of many LIF studies because its spectrum is well-known and the ($A\ ^2\Sigma^+ - X\ ^2\Pi$) transition is easily accessible in the near ultraviolet (see Table 1). This radical is a simple diatomic which can be modeled spectroscopically. It also appears to be ubiquitous in flame systems and plays a major role in reaction mechanisms.

The LIF OH concentration profile (excitation beam waist on the order of 100 micron) in Figure 7 was obtained by monitoring rotational transitions relatively insensitive to temperature variations (Eckbreth 1988) as mentioned in the Experimental Section. In general, the shape of the LIF and MB/MS profiles are in good agreement. Each diagnostic, especially MB/MS, demonstrates a region near the burner surface (between 3 and 7 mm above the surface) of enhanced concentration of OH (the height above the burner surface where this feature is found is approximately the lower half of the luminous zone of the flame).

This feature may be attributed to competition between the high temperature formation of OH via the following chain-branching reactions,

$$H + O_2 \rightarrow O + OH \quad (3)$$

and

$$O + H_2 \rightarrow H + OH \quad (4)$$

with the three body reactions of

$$H + O_2 + M \rightarrow HO_2 + M \quad (5)$$

and

$$HO_2 + H + M \rightarrow 2OH + M \quad (6)$$

which are favored at lower temperature (Warnatz 1978). While the feature is not clearly observed by LIF, detection by MB/MS clearly shows a peak of intensity at this height.

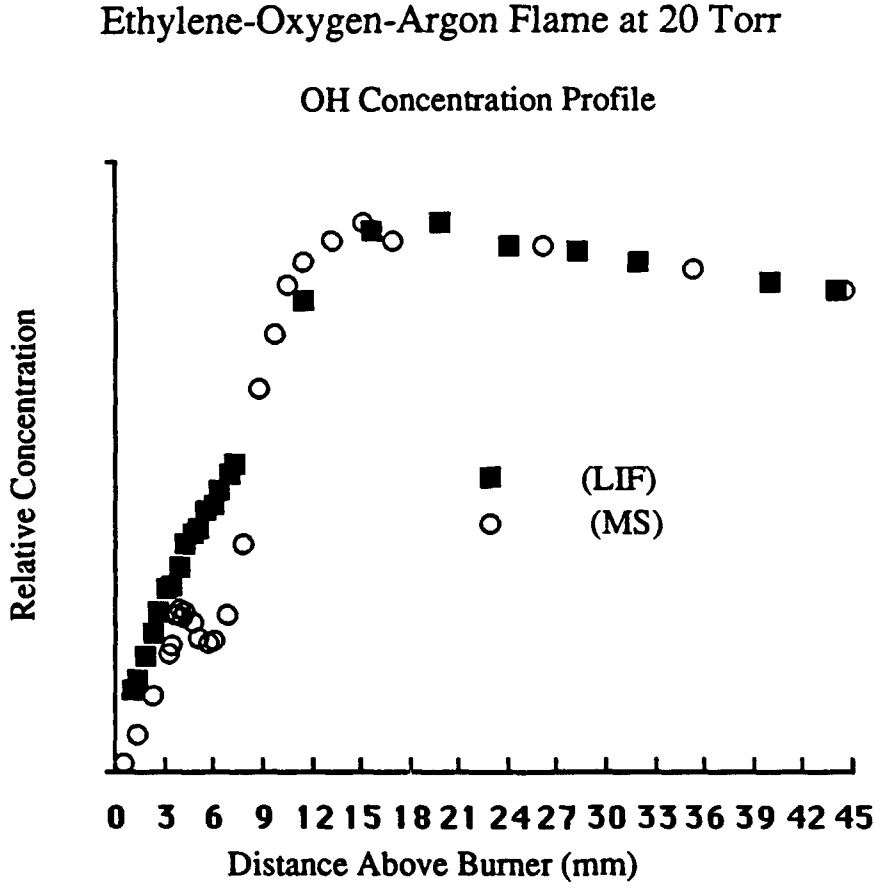

Figure 7. Species Profiles of $C_2H_4/O_2/Ar$ Flame at 20 Torr. OH Obtained by LIF (■), is Compared with that Obtained by Mass Spectrometry (O).

As with the H-atom profiles, in the preheat zone (0-7 mm) the LIF profile "leads" the MB/MS profile. The delay of the MB/MS profile relative to that generated by LIF is attributed to a lowering of the local flame temperature in the sample control volume due to the probe (Revet et al. 1978). For the comparison with the LIF technique, it is assumed that the laser probe is non-intrusive (the laser beam is heavily attenuated to avoid saturated operating conditions for the single photon excitation) in the flame environment and therefore no perturbations introduced.

Below 2 mm it is assumed, as with the case of H-atom, that as the tip of the MB/MS probe approaches the burner surface that species originating higher in the flame are less able to diffuse from around the probe tip. The concentration should then, as demonstrated in Figure 7, diminish rapidly to zero. With mass spectrometry it is therefore not possible to determine if species can back diffuse to the burner surface itself with appreciable concentrations. This artifact is contrasted with LIF at 2 mm that indicates more OH as being present near the burner surface and that the concentration is decreasing at a slower rate than the MB/MS measurement.

3.2.3 O-atom. In Figure 8 are shown the profiles for O-atom (excitation laser beam waist on the order of 100 micron). As with H-atom and OH, both detection methods agree well in the burned gas region. Near the surface, as with OH, a peak of enhanced O-atom concentration is found with MB/MS and not with LIF. Since this feature was well-pronounced in the OH profile, an attempt was made to determine if it was produced by electron-impact ionization of OH. The nominal electron energy was lowered from 17 eV ±0.5 eV FWHM (sufficiently low to prevent formation of OH from H_2O) to 13.6 eV, the threshold for forming $O^+(^4S_{3/2})$ from O-atom. At the lower electron energy the feature was unchanged. We therefore concluded that these features are present in both OH and O-atom profiles.

Since the MB/MS profile "leads" the LIF profile, an attempt to determine if other species such as CH_4 could contribute to the m/z = 16 signal in the preheat and flame zones. For this determination the first quadrupole was set at m/z = 16 at low resolution and CID performed in the second quadrupole with mass analysis performed by the third quadrupole. Scans of the third quadrupole had no indication of intensity at

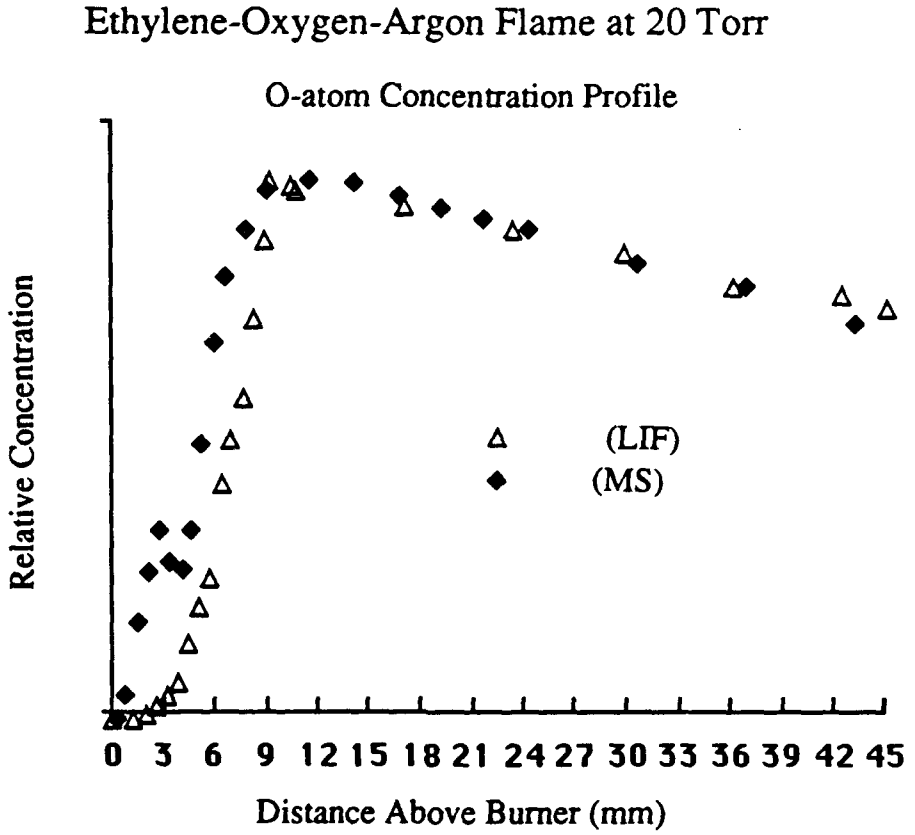

Figure 8. Species Profiles of $C_2H_4/O_2/Ar$ Flame at 20 Torr. O-Atom Obtained by LIF (△), is Compared with that Obtained by Mass Spectrometry (◆).

m/z = 12-15. The only observed signal was at m/z = 16. It was therefore concluded that the signal was indeed from O-atom. Further work is underway to determine the discrepancy in the LIF data.

The O-atom LIF profiles were determined under high photon flux conditions so as to minimize quenching effects. However, as mentioned for the H-atom case, high photon flux may lead to photochemical perturbation of the sampled volume. In addition, it is possible that O-atom LIF results may have been affected by a recently recognized phenomenon that is specific to three-level systems such as O-atom two-photon LIF, namely, amplified spontaneous emission (ASE) (Alden et al. 1989). In this situation, a population inversion can be created between the two-photon pumped $2p^3 3p\ ^3P$ upper state and the lower $3s\ ^3S$ state to which it fluoresces such that the normal LIF signal will be depleted in favor of ASE signal which will be emitted along

the direction of the incident laser beam and not collected by the detector. The ASE potential problem should be a function of total O-atom population as well as of laser pump energy, which would argue that it would be greater in the flame zone region (where O-atom concentrations are highest) rather than in the preheat region. Unfortunately, the opposite is observed, thereby indicating that at the pump energies involved that the relative proportion of the signal attributable to ASE is more dependent upon photon flux. Clearly, these considerations indicate some of the difficulties and uncertainties with regards to quantifying the optical diagnostic techniques.

4. SUMMARY

A detailed flame structure comparison between optical and mass spectrometric techniques has been presented for the species H, OH and O for a stoichiometric $C_2H_4/O_2/Ar$ flame at 20 Torr. Also described in this report is a new versatile low-pressure burner system for studies of propellant-like flames. The instrument combines different diagnostic tools to determine species concentration profiles in premixed laminar flames. Qualitatively there is good agreement between optical and molecular beam mass spectrometric techniques. These three species profiles indicate that the quartz sampler for MB/MS does not grossly affect the flame structure. However, they do indicate that backward diffusion at the burner surface is prevented by the sampler's physical presence and that measurements at or on the surface of the burner are not possible for MB/MS. However, comparison of results measured by laser-based diagnostics and by MB/MS of the $C_2H_4/O_2/Ar$ flame at 20 Torr invoke confidence concerning the validity of using MB/MS profile data for flame structure elucidation and model validation. The data also help refine the operating ranges of each technique. Even though the techniques were shown to be equivalent in the burned gas region, differences in concentration profiles were noted in preheat and flame front zones. It was also noted that whereas MB/MS can monitor H-atom, O-atom and OH concurrently, LIF and REMPI were of necessity performed separately for each radical with a greater expenditure of time.

5. REFERENCES

Alden, M., Westblom, U. and Goldsmith, J. E. M., Opt. Lett., Vol. 14, p. 305, 1989.

Balakhnin, V. P., Vandooren, J. and Van Tiggelen, P. J., Combust. Flame, Vol. 28, p. 165, 1977.

Biordi, J. C., Lazzara, C. P. and Papp, J. F., Combust. Flame, Vol. 21, p. 371, 1973.

Bittner, J., Kohse-Hoinghaus, K., Meier, U. and Just, T., Chem. Phys. Lett., Vol. 143, p. 571, 1988.

Cattolica, R. J. and Mataga, T. G., Chem. Phys. Lett., Vol. 182, p. 623, 1991.

Eckbreth, A. C., Laser Diagnostics for Combustion Temperature and Species, Abacus, Cambridge; 1988.

Foner, S. N. and Hudson, R. L., J. Chem. Phys., Vol. 21, p. 1374, 1953.

Goldsmith, J. E. M., Appl. Optics., Vol 26, p. 3566, 1987.

Goldsmith, J. E. M., Miller, J. A., Anderson, R. J. M. and Williams, L. R., Twenty-Third Symposium (Int.) on Combustion, The Combustion Institute, 1990; p 1821.

Greene, F. T., Brewer, J. and Milne, T. A., J. Chem. Phys., Vol 40, p. 1488, 1964.

Homann, K. H., Mochizuki, M. and Wagner, H. G., Z. Phys. Chem., Vol 37, p. 209, 1963.

Miziolek, A. W. and DeWilde, M. A., Optics Lett., Vol. 9, p. 390, 1984.

Puechberty, D. and M. J. Cottereau, M. J., Combust. Flame, Vol. 51, p. 299, 1983.

Rosier, B., Gicquel, P., Henry, D. and Coppalle, A., Appl. Optics, Vol. 27, p. 360, 1988.

Sausa, R. C., Howard, S. L., Locke, R. J., Kotlar, A. J. and Miziolek, A. W., Appl. Spect., submitted, 1991.

Vandooren, J., Peeters, J. and Van Tiggelen, P. J., Fifteenth Symposium (Int.) on Combustion, The Combustion Institute, 1974; p. 745.

INTENTIONALLY LEFT BLANK

No. of Copies	Organization
2	Administrator Defense Technical Info Center ATTN: DTIC-DDA Cameron Station Alexandria, VA 22304-6145
1	Commander U.S. Army Materiel Command ATTN: AMCAM 5001 Eisenhower Ave. Alexandria, VA 22333-0001
1	Commander U.S. Army Laboratory Command ATTN: AMSLC-DL 2800 Powder Mill Rd. Adelphi, MD 20783-1145
2	Commander U.S. Army Armament Research, Development, and Engineering Center ATTN: SMCAR-IMI-I Picatinny Arsenal, NJ 07806-5000
2	Commander U.S. Army Armament Research, Development, and Engineering Center ATTN: SMCAR-TDC Picatinny Arsenal, NJ 07806-5000
1	Director Benet Weapons Laboratory U.S. Army Armament Research, Development, and Engineering Center ATTN: SMCAR-CCB-TL Watervliet, NY 12189-4050
(Unclass. only) 1	Commander U.S. Army Armament, Munitions, and Chemical Command ATTN: AMSMC-IMF-L Rock Island, IL 61299-5000
1	Director U.S. Army Aviation Research and Technology Activity ATTN: SAVRT-R (Library) M/S 219-3 Ames Research Center Moffett Field, CA 94035-1000
1	Commander U.S. Army Missile Command ATTN: AMSMI-RD-CS-R (DOC) Redstone Arsenal, AL 35898-5010

No. of Copies	Organization
1	Commander U.S. Army Tank-Automotive Command ATTN: ASQNC-TAC-DIT (Technical Information Center) Warren, MI 48397-5000
1	Director U.S. Army TRADOC Analysis Command ATTN: ATRC-WSR White Sands Missile Range, NM 88002-5502
1	Commandant U.S. Army Field Artillery School ATTN: ATSF-CSI Ft. Sill, OK 73503-5000
2	Commandant U.S. Army Infantry School ATTN: ATZB-SC, System Safety Fort Benning, GA 31903-5000
(Class. only) 1	Commandant U.S. Army Infantry School ATTN: ATSH-CD (Security Mgr.) Fort Benning, GA 31905-5660
(Unclass. only) 1	Commandant U.S. Army Infantry School ATTN: ATSH-CD-CSO-OR Fort Benning, GA 31905-5660
1	WL/MNME Eglin AFB, FL 32542-5000
	Aberdeen Proving Ground
2	Dir, USAMSAA ATTN: AMXSY-D AMXSY-MP, H. Cohen
1	Cdr, USATECOM ATTN: AMSTE-TC
3	Cdr, CRDEC, AMCCOM ATTN: SMCCR-RSP-A SMCCR-MU SMCCR-MSI
1	Dir, VLAMO ATTN: AMSLC-VL-D
10	Dir, USABRL ATTN: SLCBR-DD-T

No. of Copies | Organization

4 Commander
U.S. Army Research Office
ATTN: R. Ghirardelli
D. Mann
R. Singleton
R. Shaw
P.O.Box 12211
Research Triangle Park, NC 27709-2211

2 Commander
U.S. Army Armament Research,
Development, and Engineering Center
ATTN: SMCAR-AEE-B, D. S. Downs
SMCAR-AEE, J. A. Lannon
Pinatinny Arsenal, NJ 07806-5000

1 Commander
U.S. Army Armament Research,
Development, and Engineering Center
ATTN: SMCAR-AEE-BR, L. Harris
Pinatinny Arsenal, NJ 07806-5000

1 Office of Naval Research
Department of the Navy
ATTN: R. S. Miller, Code 432
800 N. Quincy Street
Arlington, VA 22217

5 Commander
Naval Research Laboratory
ATT: M. C. Lin
J. McDonald
E. Oran
J. Shnur
R. J. Doyle, Code 6110
Washington, DC 20375

1 Superintendent
Naval Postgraduate School
Dept. of Aeronautics
ATTN: D. W. Netzer
Monterey, CA 93940

1 AFOSR
ATTN: J. M. Tishkoff
Bolling Air Force Base
Washington, DC 20332

1 University of Dayton Research Institute
ATTN: D. Campbell
AL/PAP
Edwards AFB, CA 93523

1 NASA
Langley Research Center
Langley Station
ATTN: G. B. Northam/MS 168
Hampton, VA 23365

No. of Copies | Organization

1 Aerojet Solid Proopulsion Co.
ATTN: P. Micheli
Sacramento, GA 95813

1 Applied Combustion Technology, Inc.
ATTN: A. M. Varney
P. O. Box 607885
Orlando, FL 32860

1 Atlantic Research Corp.
ATTN: R. H. W. Waesche
7511 Wellington Road
Gainesville, VA 22065

1 AVCO Everett Research
Laboratory Division
ATTN: D. Stickler
2385 Revere Beach Parkway
Everett, MA 02149

1 Battelle
ATTN: TACTEC Library, J. Huggins
505 King Avenue
Columbus, OH 43201-2693

1 Battelle Northwest Laboratories
ATTN: A. L. Rockwood, MS P-8-19
P.O. Box 999
Richland, WA 99352

1 Exxon Research & Eng. Co.
ATTN: A. Dean
Route 22E
Annandale, NJ 08801

1 General Applied Science Laboratories, Inc.
77 Raynor Avenue
Ronkonkama, NY 11779-6649

1 General Electric Ordnance Systems
ATTN: J. Mandzy
100 Plastics Avenue
Pittsfield, MA 01203

1 General Motors Rsch Labs
Physical Chemistry Department
ATTN: T. Sloane
Warren, MI 48090-9055

2 Hercules, Inc.
Allegheny Ballistics Lab.
ATTN: W. B. Walkup
E. A. Yount
P. O. Box 210
Rocket Center, MV 26726

No. of Copies	Organization
1	Alliant Techsystems, Inc. ATTN: R. E. Tompkins MN38-3300 5700 Smetana Drive Minnetonka, MN 55343
1	IBM Corporation ATTN: A. C. Tam Research Division 5600 Cottle Road San Jose, CA 95193
1	IIT Research Institute ATTN: R. F. Remaly 10 West 35th Street Chicago, IL 60616
2	Director Lawrence Livermore National Laboratory ATTN: C. Westbrook M. Costantino P. O. Box 808 Livermore, CA 94550
1	Lockheed Missiles & Space Co. ATTN: George Lo 3251 Hanover Street Dept. 52-35/B204/2 Palo Alto, CA 94304
1	Director Los Alamos National Lab ATTN: B. Nichols, T7, MS-B284 P. O. Box 1663 Los Alamos, NM 87545
1	Olin Ordnance ATTN: V. McDonald, Library P. O. Box 222 St. Marks, FL 32355-0222
1	Paul Gough Associates, Inc. ATTN: P. S. Gough 1048 South Street Portsmouth, NH 03801-5423
2	Princeton Combustion Research Laboratories, Inc. ATTN: M. Summerfield N. A. Messina 475 US Highway One Monmouth, Junction, NJ 08852
1	Hughes Aircraft Company ATTN: T. E. Ward 8433 Fallbrook Avenue Canoga Park, CA 91303

No. of Copies	Organization
2	Rockwell International Corp. Rocketdyne Division ATTN: T. L. Bunn J. E. Flanagan/HB02 6633 Canoga Avenue Canoga Park, CA 91303
1	Dow Chemical U.S.A. Analytical Sciences, Thermal Group ATTN: S. W. Froelicher 1897 Building Midland, Michigan 48667
4	Director Sandia National Laboratories Division 8354 ATTN: R. Cattolica S. Johnston P. Mattern D. Stephenson Livermore, CA 94550
1	Science Applications, Inc. ATTN: R. B. Edelman 23146 Cumorah Crest Woodland Hills, CA 91364
3	SRI International ATTN: G. Smith D. Crosley D. Golden 333 Ravenswood Avenue Menlo Park, CA 94025
1	Stevens Institute of Tech. Davidson Laboratory ATTN: R. McAlevy, III Hoboken, NJ 07030
1	Sverdrup Technology, Inc. LeRC Group ATTN: R. J. Locke, MS SVR-2 2001 Aerospace Parkway Brook Park, OH 44142
1	Thiokol Corporation Elkton Division ATTN: S. F. Palopoli P. O. Box 241 Elkton, MD 21921
3	Thiokol Corporation Wasatch Divison ATTN: S. J. Bennett P. O. Box 524 Brigham City, UT 84302

No. of Copies	Organization
1	United Technologies Research Center ATTN: A. C. Eckbreth East Hartford, CT 06108
3	United Technologies Corp. Chemical Systems Division ATTN: R. S. Brown T. D. Myers (2 copies) P. O. Box 49028 San Jose, CA 95161-9028
1	Universal Propulsion Company ATTN: H. J. McSpadden Black Canyon Stage 1 Box 1140 Phoenix, AZ 85029
1	Veritay Technology, Inc. ATTN: E. B. Fisher 4845 Millersport Highway P. O. Box 305 East Amherst, NY 14051-0305
1	Brigham Young University Dept. of Chemical Engineering ATTN: M. W. Beckstead Provo, UT 84058
1	California Institute of Technology Jet Propulsion Laboratory ATTN: L. Strand/MS 512/102 4800 Oak Grove Drive Pasadena, CA 91109
1	California Institute of Technology ATTN: F. E. C. Culick/MC 301-46 204 Karman Lab. Pasadena, CA 91125
1	University of California, Berkeley Chemistry Department ATTN: C. Bradley Moore 211 Lewis Hall Berkeley, CA 94720
1	University of California, San Diego ATTN: F. A. Williams AMES, B010 La Jolla, CA 92093
2	University of California, Santa Barbara Quantum Institute ATTN: K. Schofield M. Steinberg Santa Barbara, CA 93106

No. of Copies	Organization
1	University of Colorado at Boulder Engineering Center ATTN: J. Daily Campus Box 427 Boulder, CO 80309-0427
2	University of Southern California Department of Chemistry ATTN: S. Benson C. Wittig Los Angeles, CA 90007
1	Cornell University Department of Chemistry ATTN: T. A. Cool Baker Laboratory Ithaca, NY 14853
1	University of Delaware ATTN: T. Brill Department of Chemistry Newark, DE 19711
1	University of Florida Department of Chemistry ATTN: J. Winefordner Gainesville, FL 32611
3	Georgie Institute of Technology School of Aerospace Engineering ATTN: E. Price W. C. Strahle B. T. Zinn Atlanta, GA 30332
1	University of Illinois Department of Mechanical Engineering ATTN: H. Krier 144MEB, 1206 W. Green Street Urbana, IL 61801
1	Johns Hopkins University /APL Chemical Propulsion Information Agency ATTN: T. W. Christian Johns Hopkins Road Laurel, MD 20707
1	University of Michigan Gas Dynamics Lab Aerospace Engineering Bldg. ATTN: G. M. Faeth Ann Arbor, MI 48109-2140
1	University of Minnesota Department of Mechanical Engineering ATTN: E. Fletcher Minneapolis, MN 55455

No. of Copies	Organization
3	Pennsylvania State University Applied Research Laboratory ATTN: K. K. Kuo H. Palmer M. Micci University Park, PA 16802
1	Pennsylvania State University Department of Mechanical Engineering ATTN: V. Yang University Park, PA 16802
1	Polytechnic Institute of New York Graduate Canter ATTN: S. Lederman Route 110 Farmingdale, NY 11735
2	Princeton University Forrestal Campus Library ATTN: K. Brezinsky I. Glassman P. O. Box 710 Princeton, NJ 08540
2	Purdue University Department of Chemistry ATTN: E. Grant R. G. Cooks West Lafayette, IN 47906
2	Purdue University School of Mechanical Engineering ATTN: N. M. Laurendeau S. N. B. Murthy TSPC Chaffee Hall West Lafayette, IN 47906
1	Rensselaer Polytechnic Institute Department of Chemical Engineering ATTN: A. Fontijn Troy, NY 12181
1	Stanford University Department of Mechanical Engineering ATTN: R. Hanson Stanford, CA 94305
1	University of Texas Department of Chemistry ATTN: W. Gardner Austin, TX 78712
1	University of Utah Department of Chemical Engineering ATTN: G. Flandro Salt Lake City, UT 84112
1	Virginia Polytechnic Institute and State University ATTN: J. A. Schetz Blacksburg, VA 24061
1	University of California Los Alamos Scientific Laboratory P. O. Box 1663, Mail Stop B216 Los Alamos, NM 87545
1	Purdue University School of Aeronautics and Astronautics ATTN: J. R. Osborn Grissom Hall West Lafayette, IN 47906

INTENTIONALLY LEFT BLANK.

USER EVALUATION SHEET/CHANGE OF ADDRESS

This laboratory undertakes a continuing effort to improve the quality of the reports it publishes. Your comments/answers below will aid us in our efforts.

1. Does this report satisfy a need? (Comment on purpose, related project, or other area of interest for which the report will be used.) _____

2. How, specifically, is the report being used? (Information source, design data, procedure, source of ideas, etc.) _____

3. Has the information in this report led to any quantitative savings as far as man-hours or dollars saved, operating costs avoided, or efficiencies achieved, etc? If so, please elaborate. _____

4. General Comments. What do you think should be changed to improve future reports? (Indicate changes to organization, technical content, format, etc.) _____

BRL Report Number BRL-TR-3328 Division Symbol _____

Check here if desire to be removed from distribution list. ____

Check here for address change. ____

Current address: Organization _____
Address _____
_____

DEPARTMENT OF THE ARMY
Director
U.S. Army Ballistic Research Laboratory
ATTN: SLCBR-DD-T
Aberdeen Proving Ground, MD 21005-5066

OFFICIAL BUSINESS

BUSINESS REPLY MAIL
FIRST CLASS PERMIT No 0001, APG, MD

Postage will be paid by addressee.

Director
U.S. Army Ballistic Research Laboratory
ATTN: SLCBR-DD-T
Aberdeen Proving Ground, MD 21005-5066

NO POSTAGE
NECESSARY
IF MAILED
IN THE
UNITED STATES